Research Square

Preprints are preliminary reports that have not undergone peer review.
They should not be considered conclusive, used to inform clinical practice,
or referenced by the media as validated information.

Performance assessment for earthquake-damaged RC structure based on damaged section analysis

Juntao Ma
Dalian University of Technology
Guoxin Wang (gxwang@dlut.edu.cn)
Dalian University of Technology Faculty of Infrastructure Engineering

Research Article

Keywords: Damaged cross section analysis, Earthquake-damaged structure, RC frame structure, Performance deterioration, Fragility curve

Posted Date: March 16th, 2022

DOI: https://doi.org/10.21203/rs.3.rs-1444155/v1

License: This work is licensed under a Creative Commons Attribution 4.0 International License.
Read Full License

Performance assessment for earthquake-damaged RC structure based on damaged section analysis

Juntao Ma, Guoxin Wang*

State Key Laboratory of Coastal and Offshore Engineering, Dalian University of Technology, Dalian, Liaoning, 116024, China

Institute of Earthquake Engineering, Faculty of Infrastructure Engineering, Dalian University of Technology, Dalian, Liaoning, 116024, China

*Corresponding author at: Faculty of Infrastructure Engineering, Dalian University of Technology, No.2, Linggong Road, Dalian, 116024, China

E-mail address: gxwang@dlut.edu.cn (Guoxin Wang); majt@mail.dlut.edu.cn (Juntao Ma)

ORCID: 0000-0003-2840-2012 (Guoxin Wang)

Abstract

Evaluating quantitatively the performance of earthquake-damaged structures is significant for facilitating post-earthquake reconstruction. However, it is difficult to consider the effect of earthquake-induced damage on structure. In this paper, a new method to build earthquake-damaged structure model (EDSM) based on damaged cross section analysis (DSA) procedure is proposed. DSA can consider the effect of earthquake-induced damage on concrete and reinforcement, respectively, and determine the skeleton curve of damaged cross section. EDSM is constructed by replacing plastic hinges of structure after earthquake with trilinear skeleton curve computed by DSA. This method is realized on RC frame structure and verified by the comparison of response between undamaged structure under sequence ground motions and EDSM under the last ground motion. Subsequently, there is more prominent reduction on the vulnerability of slight limit state than higher limit states by comparing the fragility of undamaged structure and EDSM. It can be indicated that earthquake-induced damage has more significant effect on elastic properties of structure. The proposed method to establish EDSM can well represent the structure after earthquake and assess quantitatively residual performance of earthquake-damaged structure and provide a reference for reconstruction decisions.

Keywords: Damaged cross section analysis; Earthquake-damaged structure; RC frame structure; Performance deterioration; Fragility curve

1 Introduction

The earthquake, a frequent geological hazard, caused the vast casualties and economic loss in the world every year. Many structures are observed varying degree damage, rank slight to collapse, after seismic excitation. According to the field survey after Wenchuan earthquake (Tsinghua University et al. 2008), in which 54 percentages of reinforcement concrete (RC) frame structures are marked as usable, 32 percentages of RC frame structures are marked as usable after strengthening, 7 percentages of RC frame structures are marked as stop occupancy and 7 percentages of RC frame structures are marked as immediately demolish. And according to the field investigation after Lushan earthquake (Xiong et al. 2013), in which the damaged states of RC structures are divided into three grades that are L1 (usable), L2 (stop occupancy), and L3 (immediately demolish), there are 71 percentages of RC structures are marked as L1, 28 percentages for L2 and only 1 percentage for L3. Similarly, the damage states are assigned scale DS0 to DS5 in the field observation from L'Aquila after the Italy earthquake (Rossetto el al. 2011), in which there are 87 percentages of RC structures are slighter than DS2. In summary, most structures are not devastated under the ground motions, in other words, most structures are slight or moderate damage state. And, it is significant to evaluate the residual earthquake-resistant performance of not collapsed structures after earthquakes. Assessing precisely the residual performance of damaged buildings can facilitate the government carries out more reasonable measures to recover and rebuild the disaster area.

Many earthquakes have shown that earthquake-damaged structures may be damaged more severely and even collapse during following earthquakes. There is a big difference between the dynamic performance and response of an intact structure and an earthquake-damaged one, due to the reduction in the strength and stiffness of materials (e.g. concrete and steel bar) and section area during earthquake. Hatzigeorgiou and Liolios (2010) studied the nonlinear behavior of RC frame structures under repeated strong ground motions, which indicated there is a significant damage accumulation result from multiplicity of earthquakes. Wen et al. (2017) developed a framework for the vulnerability assessment of RC frame structures under mainshock-aftershock sequences, the fragility of mainshock-induced damaged structure under aftershock can be directly evaluated after obtaining the intensities of mainshock and aftershock ground motion. Burton et al. (2017) assessed the collapse capacity of earthquake-damaged structure by performing incremental dynamic analyses (IDA) to collapse. The seismic performance of

earthquake-damaged structures under aftershock ground motions is assessed by constructing ground motion sequence in literature (Burton et al. 2017; Hatzigeorgiou and Liolios 2010; Wen et al. 2017), in which dynamic response of structure under same intensity mainshock is calculated repeatedly causing a lot of time is wasted in this process.

The damaged structures after earthquake can be represented by the earthquake-damaged structure model (EDSM). The residual seismic performance of earthquake-damaged structures can be determined by evaluating the capacity of EDSM although there are difficulties in evaluating process. Williamson (2003) studied the damage-considered dynamic response of single-degree-of-freedom system under earthquake excitation based on the assumptions (Kachanov 1986; Lemaitre and Chaboche 1994) that only elastic properties could be affected by the damage, in which the damage is represented by Park-Ang damage index (Park and Ang 1985). Ou and Wu (1995) developed the method to establish the skeleton curve of damaged compression-flexure members after earthquake, in which the parameters for skeleton curve of damaged components are calculated considering the energy dissipation under earthquake excitation. There are other studies (Ludovico et al. 2013; Ou and Wu 1995; Zhou 2014;) about that the reduction in performance of components (e.g. stiffness, yield strength, yield deformation, ultimate strength, and ultimate deformation) depending on damage utilizing regression analysis. However, there is still a deficiency that is the effect of component configuration (e.g. the dimensions of section, the strength of concrete and steel bars) on the deterioration relationship is not considered. Moreover, Zhou (2014) established the EDSM by determining skeleton curve of damaged columns in soft-story, in which parameters of skeleton curve are determined by fitting equation and the Ibarra-Medina-Krawinkler model (Ibarra et al. 2005) is used to represent skeleton curve of damaged columns. In Japanese guidelines (Nakano et al. 2004), the R-index is utilized to evaluate quantitatively the damage categories of structures based on the damaged observation after earthquake, and the residual performance of component is determined depend on R-index. Subsequently, Choi et al. (2016) proposed the method to evaluate the seismic response for EDSM based on the R-index. Polese et al. (2013) defined three damage classes and damaged lumped plastic hinge model depending on damage categories, and EDSM is established to replace the extreme section of component of earthquake-damaged structure with damaged plastic hinge model. Subsequently, the capacity spectrum method (Fajifar 2000) is used to determine the capacity point of earthquake-damaged structures and then the damage-dependent vulnerability is evaluated.

It can be identified from the above introduction that the past researches still have some shortcomings

and challenges. Evaluating the impact of seismic damage on the stiffness and strength of structural members is primary obstacle to establishing EDSM. The mechanical properties of section can be evaluated quantitatively and accurately using the cross section analysis procedure, therefore, a method for constructing EDSM based on the damaged cross section analysis (DSA) procedure is proposed in this paper. Firstly, DSA is introduced in section 2. The influence of damage on concrete and steel bars and sectional dimension is considered employing fiber damage, respectively. Subsequently, the relationship of damaged section between moment and curvature is computed by using DSA. And the EDSM is established by replacing plastic hinges at both ends of components with trilinear skeleton curves obtained by DSA. Moreover, the method is realized on a three-story three-bay RC frame structure. Finally, the vulnerability of EDSM is computed and the reduction in seismic performance of EDSM is evaluated quantitatively.

2 Damaged cross section analysis (DSA)

In this section, the damage distribution and degree in the section is described by using fiber damage (FD). The effect of earthquake-induced damage on concrete and reinforcement is determined based on FD.

2.1 Fiber damage

FD is calculated based on the stress-strain history of fiber-beam element in section. The finite element model established in OpenSees (2016) employing fiber-beam element and fiber section can accurately simulate the response of RC frame structures under ground motion (Taucer et al. 1991). The method to calculate the FD of concrete fiber and steel bar fiber is introduced meticulously in literature (Ma et al. 2021). In this paper, the method is introduced curtly. The FD of concrete and steel bar is calculated by Eq. 1 and Eq. 2:

$$D_c = 1 - \frac{E_r}{E_{c0}} \tag{1}$$

where D_c is damage of concrete fiber, E_r is reload modulus of concrete, E_{c0} is the initial modulus of concrete.

$$D_s = \sum_{k=1}^{n} \frac{1}{(2N_f)_k} \tag{2}$$

where D_s is damage of steel bar fiber, $(2N_f)_k$ is the fatigue life correspond to the kth cycle half cycle, which is calculated by Eq. 3:

$$2N_f = \left(\frac{\Delta\varepsilon}{2M}\right)^{1/m} \tag{3}$$

where $\Delta\varepsilon$ is the total strain range, M and m are fatigue ductility coefficient and fatigue ductility exponent, respectively.

2.2 Influence of FD on concrete and steel bars

In the DSA, the section properties (e.g. sectional dimension, constitutive relation of concrete, area of steel bars) are affected by FD. Meanwhile, the influence of FD on concrete and steel bars fibers is considered respectively. Specifically, the area of steel bars fibers will be reduced based on FD as shown Eq. 4, the constitutive relation of concrete will be reduced based on FD as shown Eq. 5:

$$A_{sd} = \frac{\pi d^2}{4}(1 - D_s) \tag{4}$$

where A_{sd} is the area of damaged steel bar, d is the initial diameter of steel bar.

$$\sigma_{cd} = \begin{cases} 0 & \varepsilon \le \varepsilon_r \\ E_{c0}(1 - D_c)(\varepsilon - \varepsilon_r) & \varepsilon_r < \varepsilon \le \varepsilon_m \\ f_0(\varepsilon) & \varepsilon > \varepsilon_m \end{cases} \tag{5}$$

where σ_{cd} is the stress of damaged concrete fiber correspond to strain ε, ε_m is the maximum strain in history, ε_r is the strain of intersection of reload curve and abscissa axis and that is computed by Eq. 6, $f_0(\varepsilon)$ refer to undamaged concrete constitutive relation. In this paper, the concrete constitutive developed by Yassin (1994) is used as undamaged concrete constitutive relation. A comparison of constitutive between intact and damaged concrete is shown in Fig. 1.

$$\varepsilon_r = \frac{\varepsilon_m E_{c0}(1 - D_c) - \sigma_m}{E_{c0}(1 - D_c)} \tag{6}$$

where σ_m is stress correspond to ε_m.

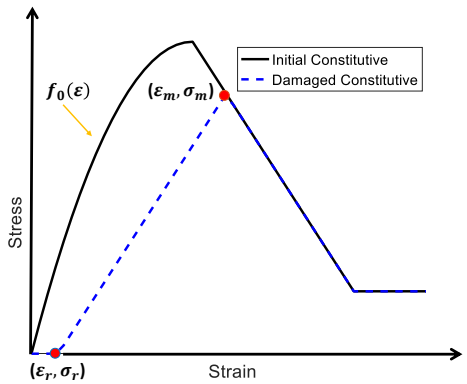

Figure 1. Schematic diagram of damaged concrete constitutive.

2.3 The procedure of damaged section analysis

The damaged section properties are determined based on the work in section 2.1 and 2.2. The ultimate bending bearing capacity M_u and ultimate curvature ϕ_u of damaged section are calculated based on the method developed by Ma et al. (2021). Following four assumptions are employed when calculating M_u and ϕ_u:

(1) Plane section assumption;

(2) The tensile strength of concrete is neglected;

(3) The ultimate status of section is reached when the strain of outermost concrete in the compression zone is equal to ultimate compressive strain;

(4) The position of steel bars in damaged section is same as that in intact section.

After computing M_u and ϕ_u, DSA is executed as follows:

Step 1: Defining the increment of curvature $\Delta\phi$ and *i*th step curvature $\phi_i = \Delta\phi \cdot i$;

Step 2: Assuming compression zone height, x_0(Fig. 2);

Step 3: Determining the strain of fibers based on plane section assumption as Eq. 7;

$$\varepsilon_m = y_m \phi_i \tag{7}$$

Where ε_m is strain of *m*th fiber, y_m is distance between *m*th fiber and neutral axis.

Step 4: Determining the stress of concrete fibers and steel bars fibers based on damaged constitutive and intact constitutive (mentioned in section 2.2), respectively.

Step 5: Calculating the internal force in section N_{in} as Eq. 8, the tensile stress of the concrete in tensile zone is ignored;

$$N_{in} = \sum \sigma_{cd} A_{c0} + \sum \sigma_s A_{sd} \tag{8}$$

Where σ_{cd} is stress of damaged concrete fiber, A_{c0} is initial area of concrete fiber, σ_s is stress of reinforcement fiber.

Step 6: The internal force is compared with external force, N_{ex}. If $|N_{in} - N_{ex}| \leq tol$ (tol is the allowable error), go to step 7, otherwise, return to step 2;

Step 7: Calculating bending moment, M_i. Start *i*+1 process, return to step 1.

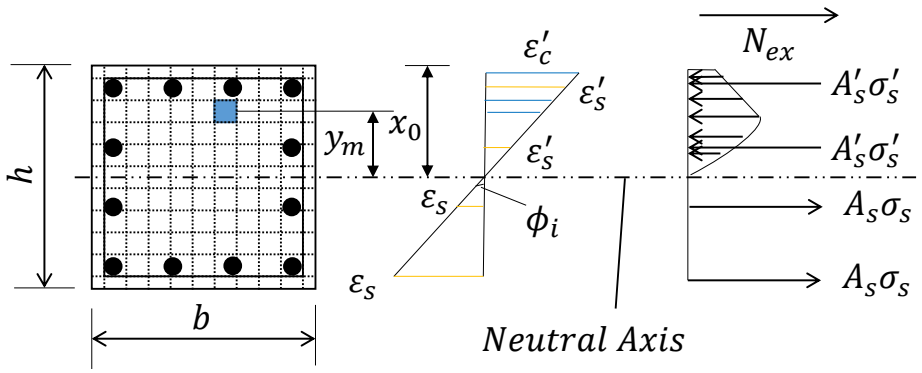

Figure 2. Section strain distribution in ultimate state.

The relationship between moment and curvature of damaged section is obtained based on the DSA introduced above. To construct EDSM, the moment and curvature relationship is transformed to a trilinear skeleton curve a shown in Fig. 3. There are three key points on the skeleton curve. Point U refers to the ultimate point and that is determined by peak point at moment-curvature relationship. And point Y refers to the yield point, which is obtained based on the same energy absorption capacity (Fig. 3) (Powell and Allahabadi 1988) for the members whose yield point cannot be observed clearly. Moreover, point R is determined on the basis of moment level of 40% yield point (i.e. $M_r = 0.4M_y$) due to generally there is a distinct change in stiffness correspond to this point (Haselton and Liel 2016). It can be seen that the relationship between moment and curvature can be well described by the deterministic trilinear skeleton curve.

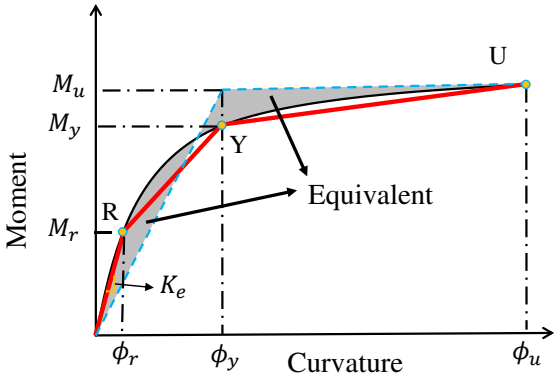

Figure 3. Defined trilinear skeleton curve.

3 Earthquake-damaged structure model (EDSM)

The field investigation after earthquake (Rossetto et al. 2011; Tsinghua University et al. 2008; Xiong et al. 2013) indicated that seismic damage of RC frame structures always concentrates on the ends of beam and column. Earthquake-induced damage can be represented by the reduction of skeleton curve for

plastic zone located ends of beams and columns. In this paper, the damaged beams and columns of structure are replaced with the elements with hinges in ESDM. Skeleton curves of plastic hinges in the damaged members are obtained by using DSA. The procedure to build EDSM as follows (Fig. 4):

Step 1: Establishing intact finite element model and exerting seismic excitation;

Step 2: Extracting stress and strain of fiber-beam element at both ends of all beams and columns, and determining the damage of concrete and reinforcements fiber in the calculated sections;

Step 3: Running DSA for sections at both ends in structure based on the fiber damage. Due to earthquake-induced damage being always asymmetrical, it is necessary to perform DSA for different directions, respectively. It is a merit of the proposed method that the effect of earthquake-induced damage on different directions of backbone curves can be considered respectively so that dynamic response of earthquake-damaged structures can be simulated more accurately.

Step 4: Employing elements with hinges to substitute damaged beams and columns, the constitutive of plastic zones is characterized by skeleton curve computed by using DSA. And the sections of element interior for beams and columns are the same as the sections in intact structure. In finally, EDSM is constructed successfully based on the steps proposed above.

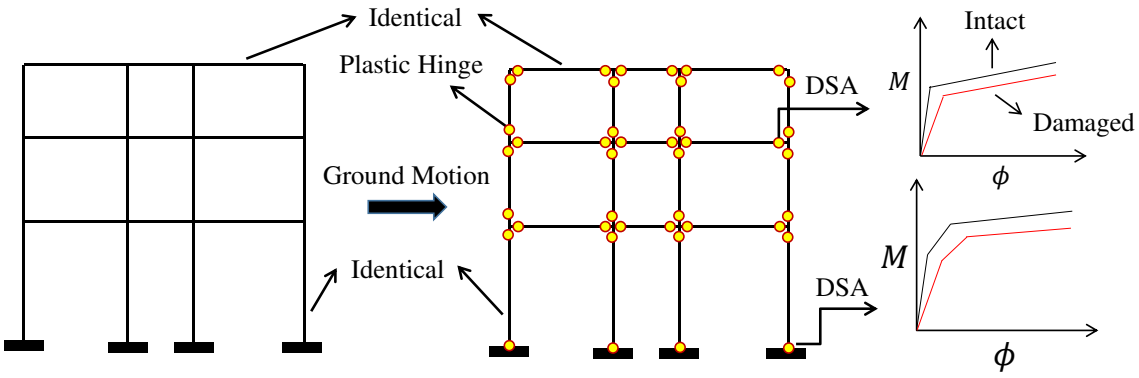

Figure 4. The flowchart of establishing EDSM.

4 Verification on EDSM

In this section, a three-story RC frame structure is designed based on Chinese buildings standards (GB-50011 2010; GB-50009 2012; GB-50010 2015). And the undamaged structure model (UDSM), EDSM and verification of EDSM are introduced, respectively.

4.1 UDSM

A three-story three-span RC frame structure is designed based on Chinese buildings standards [26-28], in which a frame is selected to analyze and establish UDSM. The elevation of selected frame is shown in Fig .5 and configurations of section and reinforcement are shown in Table 1. The design site type is class Ⅱ.Columns and beams have cover thickness of 35mm. Concrete has compressive strength of 23.4MPa and longitudinal reinforcements have yield strength of 400MPa and ultimate strength of 540MPa, and transverse reinforcements have yield strength of 335MPa and ultimate strength of 455MPa. Longitudinal and transverse steel bars have elastic modulus of 200GPa and hardening ratio of 0.01.

The finite element model of selected frame, shown in Fig. 5, is established in the OpenSees. The force-based beam-column element with fiber section, forceBeamColumns, is employed to simulate columns and beams. Moreover, the plastic behavior of the columns is concentrated in the plastic zone at ends of columns, the length of plastic zone is defined based on empirical formula as shown Eq. 9 (Paulay and Priestley 1993):

$$l_p = 0.08L + 0.022 f_y d_b \tag{9}$$

Where l_p is the length of plastic zone, L is the length of the column, f_y and d_b are the yield strength and diameter of the longitudinal reinforcements. The concrete is represented employing Concrete02 material (Yassin 1994), which can consider the confined effect of transverse reinforcement. The steel bars are modeled using Steel02 material (Filippou et al. 1983). The rebar slip and bar-buckling are not considered in this paper.

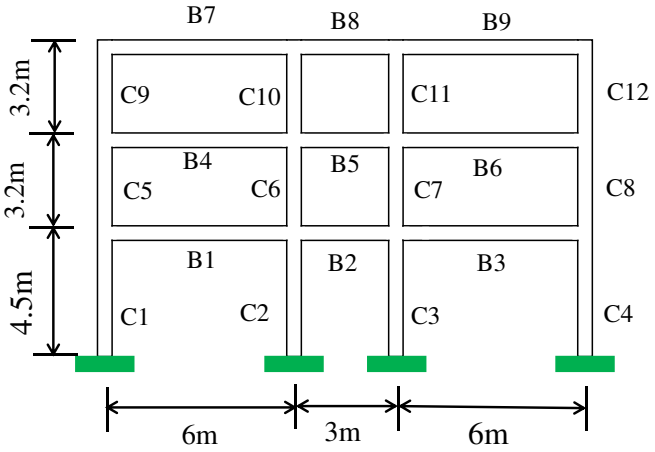

Figure 5. The elevation of designed structure.

231 Table 1. The configuration of section and steel bars of beams and columns.

Component	Section		Longitudinal Reinforcement	Transverse Reinforcement
	Width (mm)	Height (mm)		
C1-C12	500	500	10Φ[a]18	Φ8@100/150
B1, B3,B4,B6	250	500	Top: 3Φ20 Bottom: 4Φ16	Φ8@200
B2,B5	250	500	Top: 3Φ20 Bottom: 2Φ16+2Φ14	Φ8@200
B7	250	500	Top: 3Φ20 Bottom: 2Φ25	Φ8@200
B8	250	500	Top: 3Φ20 Bottom: 2Φ16	Φ8@200

232 a: The diameter of steel bars.
233

234 4.2 EDSM

235 For obtaining earthquake-damaged structure, the IMPVALL/I-ELC180 acceleration time series
236 obtained from 1940 El Centro earthquake at the Arrary #9 station is applied. And acceleration time-
237 history and response spectrum with 5% damping ratio of adoptive El Centro ground motion are shown
238 in Fig. 6. There is a minor difference between intact structure and minor damaged structure in dynamic
239 response. In this paper, El Centro ground motion is scaled by a factor of 3 to obtain earthquake-damaged
240 structure.

241 The damage of fiber-beam element of sections at both ends is calculated based on equations
242 mentioned in section 2.1. Fiber-beam element damage of C1S1 and B1S1 is shown in Fig. 7, in which
243 “C1” or “B1” is number of columns or beams (Fig. 5), respectively, moreover, “S1” refers to bottom end
244 for column or left end for beam and “S6” refers to top end for column or right end for beam. It can be
245 identified that damage of components is asymmetrical under ground motion. Particularly, the damage of
246 concrete is concentrated at the bottom of the section for B1S1. Meanwhile, the longitudinal reinforcement
247 in beams is asymmetrical. Therefore, it is necessary to assess effect of earthquake-induced damage on
248 positive and negative direction skeleton curves, respectively.

249 For constructing EDSM, DSA is performed for every sections at ends. Figure 8 shows the skeleton
250 curves of damaged and intact sections for C1S1 and B1S1, and parameters to determine skeleton curve
251 for all ends in structure are listed in Table A.1 and Table A.2 of appendix. The positive and negative
252 skeleton curves of intact column section are same due to symmetric reinforcement. And the positive and
253 negative skeleton curves of damaged column section are different due to the asymmetric damage.
254 Meanwhile, the positive and negative skeleton curves of intact beam section are different due to

asymmetric reinforcement. The negative skeleton curve of damaged beam section is approximately same as that of intact beam section due to there be almost no damage to the concrete at the top of section. It can be clearly that the properties of negative skeleton curve of damaged beam section are reduced less that positive (Table A.2) due to little damage of concrete at the top of section. And it can be identified from Table A.1 and A.2 that the elastic properties (e.g. K_e) of the components is affected dramatically by fiber damage. On the contrary, the plastic properties (e.g. Φ_u and M_u) of components is affected slightly. For establishing EDSM, hysteretic material (Fig. 9), which can consider damage due ductility and energy and degraded unloading stiffness based on ductility, is used to model plastic hinges in beam-column element based on calculating skeleton curve parameters (Table A.1 and A.2).

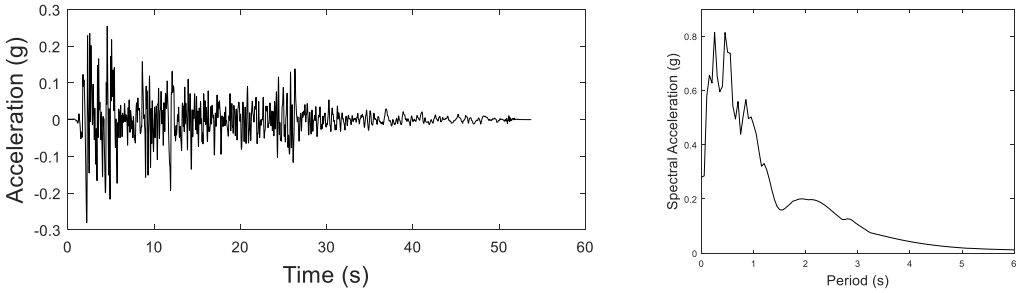

(a) (b)

Figure 6. (a) Acceleration time-history; (b) Response spectrum.

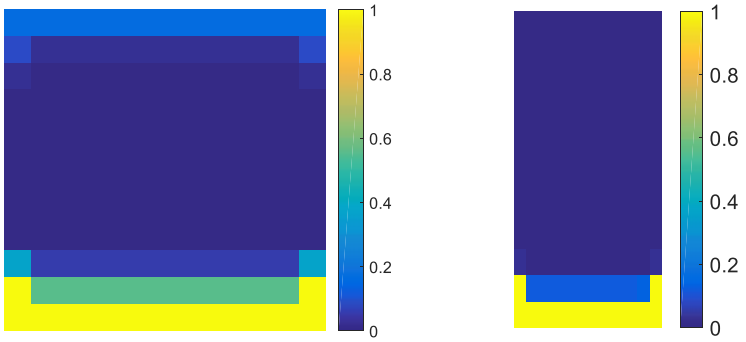

(a) (b)

Figure 7. Damage distribution of plastic hinges; (a) C1S1; (b) B1S1.

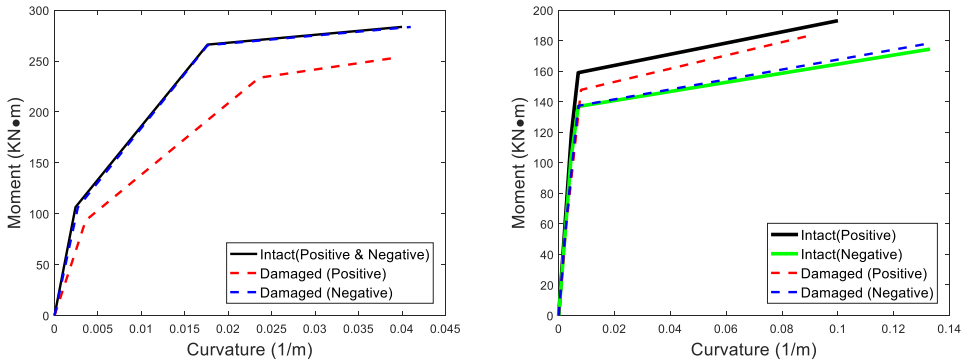

(a) (b)

Figure 8. Comparison of skeleton curve between intact and damaged section; (a) C1S1; (b) B1S1.

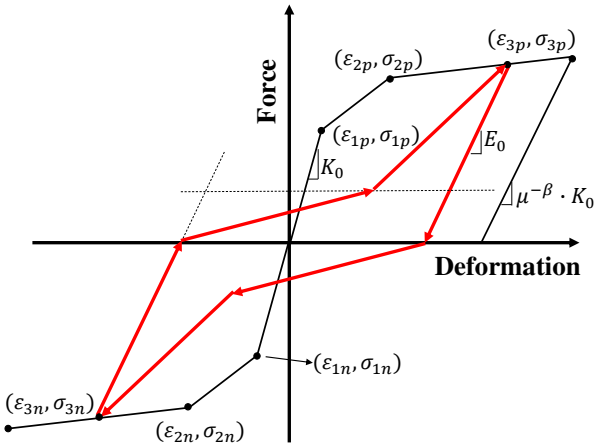

Figure 9. Hysteretic material.

For verifying EDSM constructed in this section, a comparison between response of UDSM under sequence ground motions and that of EDSM under single ground motion is finished. Sequence ground motion is generated by adding 20s zero points between El Centro and Hector ground motion as shown in Fig. 10. There zeros can help the structure come to rest after El Centro ground motion. The comparisons of inter-story drift ratio (IDR) among UDSM under Hector ground motion after El Centro ground motion and EDSM and UDSM under Hector ground motion are shown in Fig.11. And maximum IDR of ESDM and UDSM under Hector ground motion and USDM under sequence earthquake is shown in Fig.12. It can be identified form residual IDR at the beginning of that the damage of RC structure is prominent after scaled El Centro earthquake. The relative error of IDR of EDSM under Hector ground motion and UDSM under sequence ground motion for F1, F2 and F3 is 2%, 3.2% and 17%, respectively. The relative error of IDR of UDSM under Hector ground motion and UDSM under sequence ground motion for F1, F2 and F3 is 3.5%, 10% and 21%, respectively. It is clear that dynamic response of structure under the last ground motion can be well predicted by EDSM established and the method proposed in this paper is valid. And it is necessary to consider earthquake-induced damage during evaluating performance of earthquake-damaged structure.

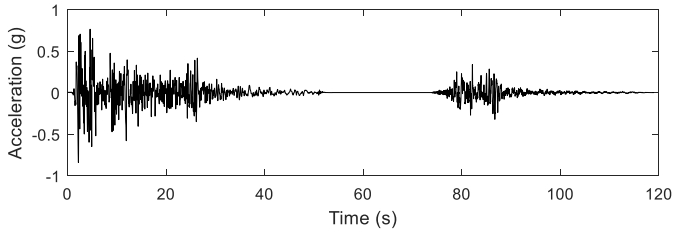

Figure 10. Sequence earthquake consisting of El Centro and Hector ground motions.

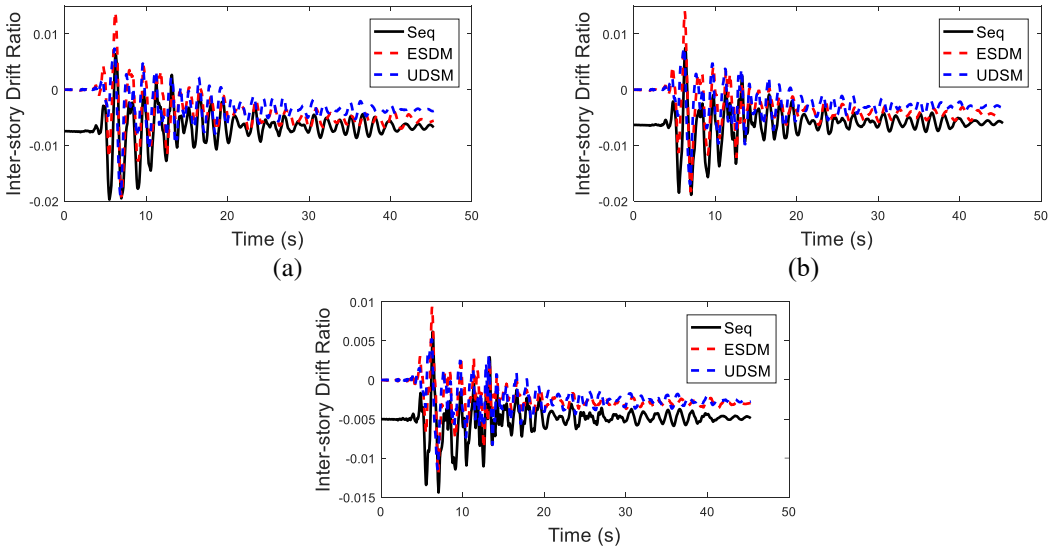

Figure 11. Comparison of IDR among ESDM and UDSM under Hector ground motion and USDM under sequence earthquake; (a) First floor; (b) Second floor; (c) Third floor.

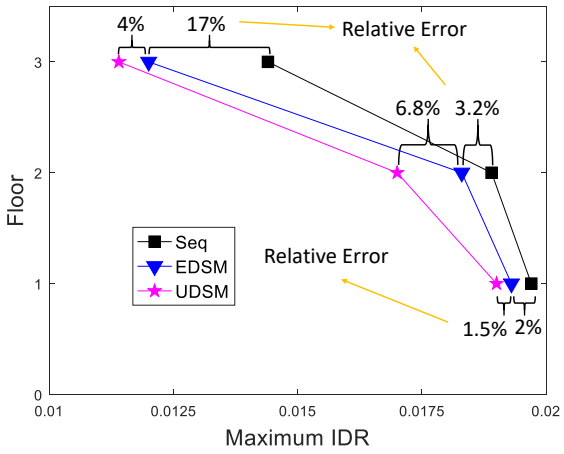

Figure 12. Maximum IDR of ESDM and UDSM under Hector ground motion and USDM under sequence earthquake

5 Performance evaluation of EDSM

5.1 Vulnerability function

For evaluating performance of EDSM, the vulnerability of EDSM and UDSM is compared. Structural vulnerability is described as a conditional probability that a certain limit state is exceeded for a given seismic intensity measure. Fragility curve can be expressed as shown Eq. 10:

$$F_R(x) = P\left[EDP \geq EDP_{LS_i} | IM = x\right] \tag{10}$$

where $F_R(x)$ is structural fragility function, EDP is engineering demand parameter of structure under ground motion and IDR is widely used as EDP, EDP_{LS_i} is the threshold of EDP for *i*th limit state of

structure, IM is ground motion intensity measure, and the spectral acceleration S_a correspond to fist-order period with 5% damping and peak ground acceleration (PGA) are widely used as IM (Burton et al. 2017; Cornell et al. 2002; Wen et al. 2017; Zareian et al. 2010). The predicted median of seismic demand of structure for a given IM can is obtained by Eq. 11 (Cornell et al. 2002):

$$ln(m_{D|IM}) = \beta_0 + \beta_1 ln(IM) \tag{11}$$

where $m_{D|IM}$ is the median of seismic demand, β_0 and β_1 are determined by a linear regression analysis of ln(EDP) and ln(IM) obtained by IDA. The dispersion $\beta_{D|IM}$ between predicted seismic demand and seismic demand computed by IDA is calculated by Eq. 12:

$$\beta_{D|IM} = \sqrt{\frac{\sum_{i=1}^{N}\left(\ln(EDP_i) - ln\left(m_{D|IM}^{i}\right)\right)^2}{N-2}} \tag{12}$$

where N is number of data computed by IDA, EDP_i and $m_{D|IM}^{i}$ are seismic demand computed by simulation and predicted seismic demand correspond to *i*th IM, respectively. Furthermore, assuming the response of structure follows the lognormal distribution, probability that seismic demand exceeds certain limit state conditioned on certain seismic intensity can be calculated by Eq. 13:

$$P\left[EDP \geq EDP_{LS_i} | IM = x\right] = 1 - \Phi\left[\frac{ln\left(EDP_{LS_i}\right) - ln\left(m_{D|IM}\right)}{\beta_{D|IM}}\right] \tag{13}$$

where $\Phi[\cdot]$ is the cumulative normal distribution function.

5.2 Fragility analysis for EDSM

Totally, 20 ground motion recordings are selected from ATC-63 (2009) strong ground motion data sets on the basis of the average shear wave velocity of 30m topsoil (Vs30) ranging 350~750 m/s correspond to the class II site (Cao 2013) in the Chinese building code. The information of selected ground motions is shown in Table 2. The response spectrum of selected ground motions are shown in Fig. 13.

Table 2. Information of selected ground motions.

Number	Event	Year	Station	R_{jb}(KM)	Vs30(m/s)	Magnitue	PGA(g)
1	Hector Mine	1999	Hector	10.3	685	7.1	0.34
2	Kobe Japan	1995	Nishi-Akashi	7.1	609	6.9	0.51
3	Kocaeli Turkey	1999	Arcelik	10.6	523	7.5	0.22
4	Friuli-Italy-01	1976	Tolmezzo	15	424	6.5	0.35
5	Northridge-01	1994	Beverly Hills-14145 Mulhol	9.4	356	6.7	0.52
6	Landers	1992	Yermo Fire Station	23.6	354	7.3	0.24

7	Loma Prieta	1989	Gilroy Array #3	12.2	350	6.9	0.56
8	Gazli-USSR	1976	Karakyr	3.9	660	6.8	0.72
9	Nahanni-Canada	1985	Site 1	2.5	660	6.8	1.10
10	Nahanni-Canada	1985	Site 2	0	660	6.8	0.49
11	Cape Mendocino	1992	Cape Mendocino	0	513	7	1.50
12	Loma Prieta	1989	Corralitos	0.1	462	6.9	0.64
13	Northridge-01	1994	LA-Sepulveda VA Hospital	0	380	6.7	0.93
14	Loma Prieta	1989	BRAN	3.9	377	6.9	0.53
15	Tabas Iran	1978	Dayhook	0	471	7.4	0.41
16	Duzce Trukey	1999	Lamont 531	8.03	638	7.1	0.16
17	Irpinia Italy-01	1980	Calitri	13.34	456	6.9	0.14
18	Montenegro Yugoslavia	1979	Pertovac-Hotel Olivia	0	543	7.1	0.46
19	Manjil Iran	1990	Abbar	12.55	724	7.4	0.5
20	Chi-Chi Taiwan	1999	TCU067	0.62	434	7.6	0.5

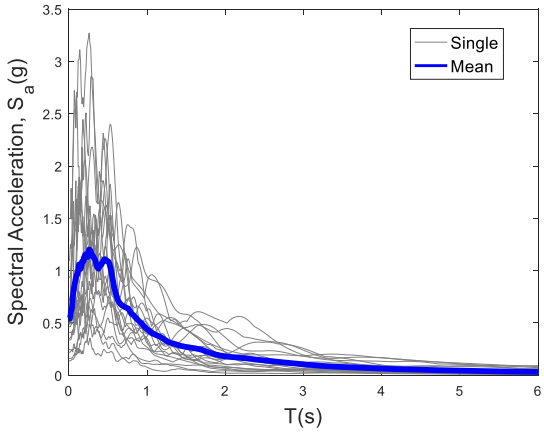

Figure 13. Response spectrum of significant and total duration ground motions.

On the basis of formulation mentioned above, IDA for UDSM and EDSM under selected ground motions is performed. Maximum inter-story drift ratio and peak ground acceleration (PGA) are selected as engineering demand parameter and intensity measure, respectively. Hazus (FEMA 2006) determined median values of IDR at the threshold of structural damage for varied structure types and rises. And Lin et al. (2010) developed the mapping of seismic design level between Chinese code and Hazus. The threshold of IDR of limit state for three-story RC frame structures designed in this paper is list in Table 3. The IDA curves of UDSM and EDSM under selected earthquakes are shown in Fig. 14. And the mean PGA of varies limit state for UDSM and EDSM is shown in Table 4. Mean PGA of EDSM for four limit states is 10%, 16%, 12%, 7% smaller than that of UDSM, respectively. Earthquake-induced damage results in a reduction in structural performance due to reduction in stiffness and strength of components after earthquake. Meanwhile, the impact of damage on complete damage state is milder than other

damage state.

The vulnerability parameters (i.e. β_0, β_1 and $\beta_{D|S_a}$) of UDSM and EDSM are determined by linear regression analysis as shown in Fig. 15 and Table 5. Moreover, the fragility curves of UDSM and EDSM for four limit states are shown in Fig. 16. It can be identified from Fig. 16 that EDSM is more fragile than UDSM for four limit states, which demonstrates that earthquake-induced damage has markedly influence on structural performance. For estimating quantitatively performance deterioration, performance reduction index of structure is defined as Eq. 14:

Table 3. Threshold of IDR of varies limit state.

Limit States	Slight	Moderate	Extensive	Complete
Threshold	0.004	0.006	0.016	0.04

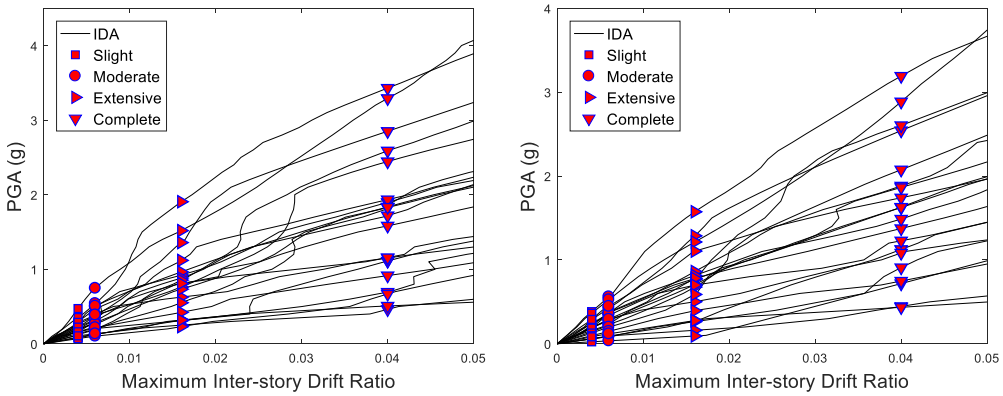

Figure 14. IDA curves; (a) UDSM; (b) EDSM.

Table 4. Mean PGA of varies limit state of UDSM and EDSM.

Type	Slight (g)	Moderate (g)	Extensive (g)	Complete (g)
UDSM	0.2	0.32	0.78	1.69
EDSM	0.18	0.27	0.69	1.58
Reduction	10%	16%	12%	7%

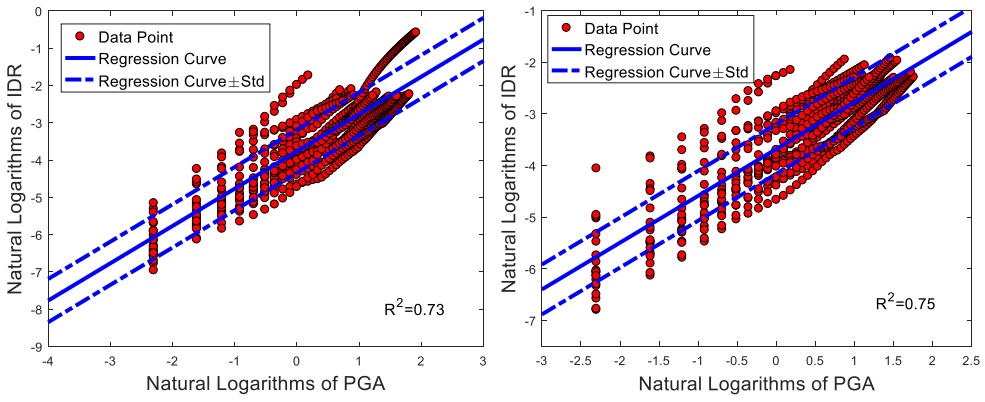

Figure 15. Regression analysis of results computed by IDA; (a) UDSM; (b) EDSM.

Table 5. The vulnerability parameters of UDSM and EDSM

Type	$\boldsymbol{\beta_0}$	$\boldsymbol{\beta_1}$	$\boldsymbol{\beta_{D|S_a}}$	$\boldsymbol{R^2}$
UDSM	-3.766	1.001	0.58	0.73
EDSM	-3.68	0.907	0.483	0.75

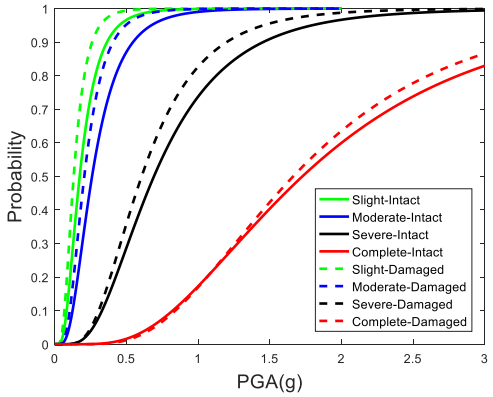

Figure 16. Comparison of fragility curve between UDSM and EDSM.

$$\gamma = 1 - \frac{IM_{EDSM}^{50\%}}{IM_{UDSM}^{50\%}} \tag{14}$$

where γ is performance reduction index, $IM_{UDSM}^{50\%}$ and $IM_{EDSM}^{50\%}$ are ground motion intensity measure corresponds to 50% exceedance probability for UDSM and EDSM, respectively. The reduction index for four limit states in shown in Table 6.

Table 6. Reduction index for four limit states.

Limit States	Slight	Moderate	Severe	Complete
γ	23.5%	19.2%	11.6%	4%

The performance of EDSM is reduced by 23.5%, 19.2%, 11.6%, 4% for slight, moderate, severe, complete limit state, respectively. It is clear that the reduction of vulnerability decreases gradually as the limit state increases. As mentioned in section 4.2, earthquake-induced damage has the severest impact on the elastic properties of structures. Necessarily, the reduction of structural performance is closely related to the degree of structural damage. Determining the relationship between the performance deterioration and degree of damage is the focus of future work.

6 Conclusion

A method to build earthquake-damaged structure model (EDSM) based on damaged cross section analysis (DSA) procedure is proposed. This method can be used to establish EDSM to represent structure after earthquake and assess the performance of structures with earthquake-induced damage. The following conclusions are drawn:

(1) Damaged cross section analysis (DSA) procedure can respectively consider effect of damage on

concrete and reinforcement and obtain the relation between moment and curvature of damaged section. Furthermore, the moment-curvature curve is transformed to a trilinear curve by identifying three key points. Earthquake-induced damage on beams and columns is generally asymmetric and DSA can consider the effect of earthquake-damaged on positive and negative direction of section, respectively.

(2) The method proposed to establish EDSM is realized on a three-story three-bay RC frame structure. By comparing among IDR of EDSM and UDSM under Hector ground motion and UDSM under sequence earthquake, it is necessary to consider effect of earthquake-induced damage on performance of structure when assessing performance of earthquake-damaged structure. And the EDSM established by the method in this paper can well represent damaged structure after earthquake.

(3) The fragility curve of EDSM is computed to quantitatively estimate the performance of earthquake-damaged structure. The EDSM is more fragile than UDSM due to reduction of stiffness and strength of members after earthquake. In this paper, the reduction of vulnerability can be quantitatively formulated by performance reduction index. Moreover, reduction of vulnerability decreases gradually as the limit state increases, that results from earthquake-induced damage has the severer effect on the elastic properties than that on plastic properties of structures. Of course, the reduction of structural performance is closely related to the degree of structural damage. Determining the relationship between the performance deterioration and degree of damage is the focus of future work.

Appendix A. Parameters for determining skeleton curve

Table A.1. Parameters of skeleton curve for column sections.

Direction	Section	K_e [a] ($10^4 KN \cdot m^2$)	ϕ_y ($1/m$)	M_y ($KN \cdot m$)	ϕ_u ($1/m$)	M_u ($KN \cdot m$)
+	C1S1	2.6(↓41%)[b]	0.024(↑34%)	234(↓12%)	0.039(↓2%)	253(↓11%)
	C1S6	4.2(↓5%)	0.018	266	0.04	284
	C2S1	2.8(↓44%)	0.016(↑33%)	233(↓13%)	0.034(↑10%)	262(↓11%)
	C2S6	4.3(↓16%)	0.012	266	0.034(↑10%)	296
	C3S1	3.3(↓35%)	0.017(↑36%)	247(↓8%)	0.031	268(↓10%)
	C3S6	3.9(↓24%)	0.012	262(↓2%)	0.034(↑10%)	296
	C4S1	3.4(↓22%)	0.018	250(↓6%)	0.038(↓5%)	284
	C4S6	3.7(↓17%)	0.018	267	0.04	284
	C5S1	3.8(↓2%)	0.017	248	0.047	269
	C5S6	3.9	0.017	248	0.047	269
	C6S1	4.0(↓4%)	0.017	259	0.046	278
	C6S6	3.7(↓12%)	0.017	259	0.046	278
	C7S1	4.0(↓5%)	0.017	259	0.046	278
	C7S6	4.0(↓5%)	0.017	259	0.046	278
	C8S1	3.9	0.017	248	0.047	269
	C8S6	3.1(↓21%)	0.017	245(↓1%)	0.048(↑2%)	270
	C9S1	3.4	0.016	232	0.061	255
	C9S6	3.4	0.016	232	0.061	255
	C10S1	3.5	0.016	237	0.059	259
	C10S6	3.1(↓13%)	0.016	235	0.05(↓15%)	259
	C11S1	3.5(↓2%)	0.016	237	0.059	259
	C11S6	3.3(↓7%)	0.016	237	0.059	259
	C12S1	3.3(↓2%)	0.016	232	0.061	255
	C12S6	3.3(↓2%)	0.016	232	0.061	255
-	C1S1	4.0(↓10%)	0.018	266	0.041(↑3%)	284
	C1S6	3.8(↓13%)	0.018	268	0.04	284
	C2S1	4.0(↓21%)	0.012	263(↓2%)	0.034(↑10%)	296
	C2S6	4.3(↓15%)	0.012	267	0.034(↑10%)	296
	C3S1	3.5(↓32%)	0.018(↑50%)	268	0.034(↑10%)	296
	C3S6	4.7(↓8%)	0.012	267	0.033(↑6%)	296
	C4S1	3.1(↓30%)	0.017	242(↓9%)	0.043(↑8%)	282
	C4S6	4.3(↓3%)	0.018	266	0.04	284
	C5S1	3.7(↓4%)	0.017	248	0.047	269
	C5S6	2.7(↓30%)	0.017	228(↓8%)	0.047	268
	C6S1	3.7(↓11%)	0.017	259	0.046	278
	C6S6	3.8(↓11%)	0.017	260	0.046	278
	C7S1	3.8(↓10%)	0.017	260	0.046	278
	C7S6	3.6(↓15%)	0.017	258	0.046	278
	C8S1	3.6(↓7%)	0.017	249	0.047	269
	C8S6	3.9	0.017	248	0.047	269
	C9S1	3.3(↓2%)	0.016	232	0.061	255
	C9S6	3.3(↓2%)	0.016	232	0.061	255
	C10S1	3.4(↓4%)	0.016	237	0.059	259
	C10S6	2.9(↓18%)	0.016	228(↓4%)	0.059	259
	C11S1	3.5	0.016	237	0.059	259
	C11S6	3.0(↓15%)	0.016	233(↓2%)	0.05(↓15%)	259
	C12S1	3.4	0.016	232	0.061	255
	C12S6	3.4	0.016	232	0.061	255

a: K_e is the stiffness of elastic stage of skeleton curve, $K_e = M_r/\phi_r$.

b: ↓ and ↑ refer to reduction and increment, respectively. And the default represents a change of less than 1%.

Table A.2. Parameters of skeleton curve for beam sections.

Direction	Section	K_e $(10^4 KN \cdot m^2)$	ϕ_y $(1/m)$	M_y $(KN \cdot m)$	ϕ_u $(1/m)$	M_u $(KN \cdot m)$
+	B1S1	2.2(↓15%)	0.008(↑14%)	148(↓7%)	0.091(↓9%)	184(↓5%)
	B1S6	2.3(↓15%)	0.008(↑14%)	152(↓5%)	0.1	190(↓2%)
	B2S1	1.8(↓15%)	0.009(↑29%)	139(↓13%)	0.071(↓25%)	164(↓14%)
	B2S6	2.1(↓15%)	0.008(↑14%)	148(↓7%)	0.054(↓43%)	178(↓7%)
	B3S1	2.2(↓15%)	0.008(↑14%)	148(↓7%)	0.097(↓3%)	186(↓4%)
	B3S6	2.3(↓15%)	0.008(↑14%)	151(↓5%)	0.089(↓11%)	188(↓3%)
	B4S1	2.1(↓15%)	0.008(↑14%)	141(↓11%)	0.099(↓1%)	178(↓8%)
	B4S6	2.2(↓15%)	0.008(↑14%)	148(↓7%)	0.1	186(↓4%)
	B5S1	2.0(↓15%)	0.008(↑14%)	128(↓20%)	0.087(↓8%)	159(↓17%)
	B5S6	2.2(↓15%)	0.008(↑14%)	151(↓5%)	0.095	185(↓3%)
	B6S1	2.1(↓15%)	0.008(↑14%)	138(↓13%)	0.1	175(↓10%)
	B6S6	2.2(↓15%)	0.008(↑14%)	149(↓6%)	0.1	186(↓3%)
	B7S1	2.4(↓15%)	0.008(↑14%)	155(↓3%)	0.121	201
	B7S6	2.4(↓15%)	0.008(↑14%)	158(↓1%)	0.121	201
	B8S1	2.4(↓15%)	0.008	159	0.064(↓4%)	180(↓3%)
	B8S6	2.3(↓15%)	0.008	157(↓1%)	0.064(↓4%)	180(↓3%)
	B9S1	2.4(↓15%)	0.008(↑14%)	155(↓3%)	0.121	201
	B9S6	2.4(↓15%)	0.008(↑14%)	158	0.121	201
-	B1S1	2.3	0.007	137	0.132(↓1%)	178(↓2%)
	B1S6	2.4	0.007	137	0.133	174
	B2S1	1.7(↓17%)	0.007	95(↓17%)	0.142	122(↓18%)
	B2S6	1.0(↓42%)	0.007	56(↓41%)	0.134(↓8%)	76(↓42%)
	B3S1	2.3	0.007	137	0.133	179(↑2%)
	B3S6	2.4	0.007	137	0.133	174
	B4S1	2.3	0.007	137	0.133	175
	B4S6	2.3	0.007	137	0.132(↓1%)	178(↑2%)
	B5S1	1.9(↓10%)	0.007	116(↓3%)	0.142	157
	B5S6	1.7(↓16%)	0.007	103(↓11%)	0.124(↓19%)	161(↑2%)
	B6S1	2.3	0.007	137	0.13(↓3%)	177(↑2%)
	B6S6	2.3	0.007	137	0.132(↓1%)	178(↑2%)
	B7S1	2.8	0.007	166	0.114	207
	B7S6	2.8	0.007	166	0.114	207
	B8S1	1.3	0.007	69	0.161(↓12%)	95
	B8S6	1.3	0.007	70	0.161(↓12%)	95
	B9S1	2.8	0.007	166	0.114	207
	B9S6	2.7	0.007	166	0.114	207

Declarations

Funding

This work was supported by the National Key Research and Development Program of China under Grant number [2018YFD1100405].

Competing Interests

The authors declare that we do not have any commercial or associative interest that represents a conflict of interest in connection with the work submitted.

Data Availability

The datasets generated during the current study and MATLAB code are available from the corresponding author on reasonable request.

References

ATC-63 (2009) Quantification of building seismic performance factors. Washington, D. C.: Applied Technology Council.

Burton HV, Sreekumar S, Sharma M, Sun H (2017) Estimation aftershock collapse vulnerability using mainshock intensity, structural response and physical damage indicators. Structural Safety 68:85-96. http://dx.doi.org/10.1016/j.strusafe.2017.05.009

Cornell CA, Jalayer F, Hamburger RO, Foutch DA (2002) Probabilistic basis for 2000 SAC federal emergency management agency steel moment frame guidelines. Journal of Structural Engineering 128(4):526-533. http://dx.doi.org/10.1061/(ASCE)0733-9445(2002)128:4(526)

Civil and Structural groups of Tsinghua University, Xian Jiaotong University, Beijing Jiaotong University (2008) Analysis on seismic damage of buildings in the Wenchuan earthquake. Journal of Building Structures 29(4):1-9. https://doi.org/10.14006/j.jzjgxb.2008.04.001

Cao JT (2013) Comparative Study on Seismic Design of Reinforced Concrete Frames between Chinese, American and European Codes. Dissertation, Xi' An University of Architecture and Technology.

Choi H, Sanada Y, Kashiwa H, Watanabe Y, Tanjung J, Jiang HY (2016) Seismic response estimation method for earthquake-damaged RC buildings. Earthquake Engineering and Structural Dynamics 45:999-1018. http://dx.doi.org/10.1002/eqe.2715

Filippou FC, Popov EP, Bertero VV (1983) Effects of Bond Deterioration on Hysteretic Behavior of Reinforced Concrete Joints. Report EERC 83-19, Earthquake Engineering Research Center, University of California, Berkeley.

Fajifar P (2000) A nonlinear analysis method for performance-based seismic design. Earthquake Spectra 16(3): 573-592. http://dx.doi.org/10.1193/1.1586128

Federal Emergency Management Agency (2006) Multi-hazard Loss Estimation Methodology Earthquake Model. Washington: D.C.

Hatzigeorgiou GD, Liolios AA (2010) Nonlinear behavior of RC frames under repeated strong ground motions. Soil Dynamics and Earthquake Engineering 30:1010-1025. http://dx.doi.org/10.1016/j.soildyn.2010.04.013

Haselton CB, Liel AB, Taylor-Lamge SC, Deierlein GG (2016) Calibration of model to simulate response of reinforced concrete beam-columns to collapse. ACI Structural Journal 113(6): 1141-1152.

https://doi.org/10.14359/51689245

Ibarra LF, Medina RA, Krawinkler H (2005) Hysteretic models that incorporate strength and stiffness deterioration. Earthquake Engineering and Structural Dynamics 34:1489-1511. http://dx.doi.org/10.1002/eqe.495

Kachanov LM (1986) Introduction to continuum damage mechanics, Martinus Nijhoff, The Netherlands.

Lemaitre J, Chaboche JL (1994) Mechanics of solid materials, Cambridge University, Cambridge, England.

Lin S, Xie LL, Gong MS, Li M (2010) Performance-based methodology for assessing seismic vulnerability and capacity of buildings. Earthquake Engineering and Engineering Vibration 9: 157-165. http://dx.doi.org/10.1007/s11803-010-0002-8

Ludovico MD, Polese M, d'Aragona MG, Prota A, Manfredi G (2013) A proposal for plastic hinges modification factors for damaged RC columns. Engineering Structures 51:99-112. http://dx.doi.org/10.1016/j.engstruct.2013.01.009

Lu PJ (2021) Research on bracing non-seismic structure and seismic damaged RC structure modeling. Dissertation, Dalian University of Technology.

Ministry of Housing and Urban-Rural Development of the People's Republic of China (2010) Code for seismic design of buildings. Beijing: China Construction Industry Press.

Ministry of Housing and Urban-Rural Development of the People's Republic of China (2012) Load code for the design of building structures. Beijing: China Construction Industry Press.

Ministry of Housing and Urban-Rural Development of the People's Republic of China (2015) Code for design of concrete structures. Beijing: China Construction Industry Press.

Ma JT, Wang GX, Lu PJ (2021) Residual bending bearing capacity assessment of reinforced concrete column under cyclic loading based on fiber-beam element. Bulletin of Earthquake Engineering 19:4339-4367. http://dx.doi.org/10.1007/s10518-021-01123-y.

Nakano Y, Maeda M, Kuramoto H, Murakami M (2004) Guideline for post-earthquake damage evaluation and rehabilitation of RC buildings in Japan. 13th world conference on earthquake engineering, Vancouver, B.C., Canada 124.

OpenSees (2019) Open system for earthquake engineering simulation. (http://opensees.berkeley.edu/).

494 Ou JP, Wu B (1995) Experimental research on restoring force of damaged compression-flexure
495 members and its applications. Journal of Building Structures 16(6):21-29. http://dx.doi.org/10.14006/j .j
496 zj gxb.1995.06.004
497 Park YJ, Ang AHS (1985) Mechanistic seismic damage model for reinforced concrete. Journal of
498 Structural Engineering 111(4):722-739. http://dx.doi.org/10.1061/(ASCE)07339445(1985)111:4(722)
499 Powell GH, Allahabadi AR (1988) Seismic damage prediction by deterministic methods: concepts
500 and procedures. Earthquake Engineering and Structural Dynamics 16:719-734.
501 https://doi.org/10.1002/eqe.4290160507
502 Paulay T, Priestley MJN (1993) Seismic Design of Reinforced Concrete and Masonry Buildings.
503 New York, USA.
504 Polese M, Ludovico MD, Prota A, Manfredi G (2013) Damage-dependent vulnerability curves for
505 existing buildings. Earthquake Engineering and Structural Dynamics 42:853-870.
506 http://dx.doi.org/10.1002/eqe.2249
507 Rossetto T, Peiris N, Alarcon JE, So E, Sargeant S, Free M, Sword-Daniels V, Re DD, Libberton C,
508 Verrucci E, Sammonds P, Walker JF (2011) Field observations from the Aquila, Italy earthquake of April
509 6, 2009. Bulletin of Earthquake Engineering 9: 11-37. http://dx.doi.org/10.1007/s10518-010-9221-7
510 Taucer FF, Spacone E, Filippou FC (1991) A fiber beam-column element for seismic response
511 analysis of reinforced concrete structures. Report No. UCB/EERC-91/17, UC Berkeley, American.
512 Williamson EB (2003) Evaluation of damage and P-Δeffects for systems under earthquake
513 excitation. Journal of Structural Engineering 129(8): 1036-1046. http://dx.doi.org/10.1061/(ASCE)0733-
514 9445(2003)129:8(1036)
515 Wen WP, Zhai CH, Ji DF, Li S, Xie LL (2017) Framework for the vulnerability assessment of
516 structure under mainshock-aftershock sequences. Soil Dynamics and Earthquake Engineering 101:41-52.
517 http://dx.doi.org/10.1016/j.soildyn.2017.07.002
518 Xiong LH, Lan RQ, Wang YM, Tian XM, Feng B (2013) Earthquake damage investigation of
519 structures in 7.0 Lushan strong earthquake. Journal of Earthquake Engineering and Engineering Vibration
520 33(04):35-43. https://doi.org/10.11810 /1000-1301.20130405
521 Yassin MHM (1994) Nonlinear analysis of prestressed concrete structure under monotonic and
522 cyclic loads. Dissertation, University of California, Berkeley.
523 Zareian F, Krawinkler H, Ibarra L, Lignos D (2010) Basis concepts and performance measures in

524 prediction of collapse of buildings under earthquake ground motions. Structural Design of Tall and
525 Special Buildings 19:167-181. http://dx.doi.org/10.1002/tal.546
526 Zhou XL (2014) Research on seismic performance evaluation method of earthquake damaged RC
527 frame structures. Dissertation, College of Civil Engineering of Chongqing University.
528